Improving the thermal and electrical properties of polymer composites by ordered distribution of carbon micro- and nanofillers

Oleksii Maruzhenko, Yevgen Mamunya, Gisèle Boiteux, Slawomira Pusz, Urszula Szeluga, Sébastien Pruvost

Improving the thermal and electrical properties of polymer composites by ordered distribution of carbon micro- and nanofillers

Oleksii Maruzhenko[a,b], Yevgen Mamunya[a], Gisèle Boiteux[c], Sławomira Pusz[d], Urszula Szeluga[d] and Sébastien Pruvost[b]*

[a] Institute of Macromolecular Chemistry NAS of Ukraine, 48, Kharkivske chaussee, Kyiv, 02160, Ukraine

[b] Univ Lyon, INSA Lyon, UMR CNRS 5223, IMP Ingénierie des Matériaux Polymères, F-69621, Villeurbanne, France

[c] Univ Lyon, Université Lyon 1, UMR CNRS 5223, IMP Ingénierie des Matériaux Polymères, F-69622, Villeurbanne, France

[d] Centre of Polymer and Carbon Materials, Polish Academy of Sciences, M. Curie-Skłodowskiej 34, Zabrze, Poland

Corresponding author:

* Univ Lyon, INSA Lyon, UMR CNRS 5223, IMP Ingénierie des Matériaux Polymères, F-69621, Villeurbanne, France. E-mail: sebastien.pruvost@insa-lyon.fr

This article presents the study of electrical and thermal properties of segregated polymer composites based on ultra-high-molecular-weight polyethylene (UHMWPE) filled with carbon fillers (nanofiller graphene (Gr), microfiller anthracite (A) and hybrid filler Gr/A). It is shown that the formation of a segregated structure with an ordered distribution of the filler leads to a high local concentration in the intergrain boundaries, which causes a lower percolation threshold. Thus, in the composite UHMWPE+A, the percolation threshold is an order of magnitude lower than for a system with a random distribution of the filler. The segregated composite with nanofiller UHMWPE+Gr provides a 14-fold lower percolation threshold than the composite with microfiller UHMWPE+A. Composite with the hybrid filler Gr/A also exhibits a low percolation threshold close to the UHMWPE+Gr. The plot of the thermal conductivity versus filler content does not show the percolation behavior and obeys the equation of the Lichtenecker. The thermal conductivity parameter λ_f in the segregated system is 4.4 times higher than for the uniform distribution of the filler that indicates an increased thermal transport through the filler phase located at the boundaries in the segregated structure.

Keywords: polymer composites; nanocomposites; segregated structure; electrical conductitivity; thermal conductivity.

1. Introduction.

Recently, conductive polymeric composites (CPCs) have been widely used in applications, which are of great interest both in the industry and in academia [1-3]. In particular, they are often used as antistatic or EMI shielding materials, sensor materials, conductive elements in microelectronics, electrodes in nomad sources of current, materials for medical equipment, etc. [4, 5]. The main advantages of such systems are a relative cheapness, a low weight, an easy processing of products with complex shape, a corrosion resistance and a controllable conductivity.

Commonly, to prepare CPCs, conductive filler particles are randomly dispersed in polymer matrix to create conductive paths. To produce composites with a wide range of electrical conductivity, particles with different nature, shape and dispersion state are used as conductive fillers (e.g. micro-/nano carbon particles such as carbon black, graphene, carbon nanotubes, etc. [6-8]). However, to obtain high values of conductivity, CPCs with random distribution of the filler require relatively high concentration of the conductive phase that leads to a complex processing and degrading mechanical properties of the composites (i.e. more brittle) and this way is not always economically reasonable.

These problems can be solved processing systems with segregated distribution of the conductive phase in the polymer matrix. In this case, filler particles are localized at the boundary between polymer grains and, consequently, local filler concentrations is much larger than the average concentration related to the total volume of a composite [9-12]. Such distribution of the filler affects different physical properties of composites [13-15]. The properties such as electrical and thermal conductivity, dielectric characteristics and certain mechanical parameters can be related to the distance between particles or the existence of contacts between them and are mostly defined by the local concentration of filler. Due to the local concentration of conductive fillers inside polymer matrix, the percolation threshold φ_c defining the insulator/conductor transition, is much lower in a segregated system than for a random distribution of filler.

George et al. demonstrated that, in the case of natural rubber, segregated systems helped to improve mechanical properties [16]. The segregated composite with 1 vol.% of carbon nanotubes showed a significant improvement of mechanical properties such as tensile strength, elongation at break, modulus of elasticity and tensile strength in comparison with unfilled matrix. Also, a relatively low percolation threshold was obtained φ_c = 0.043 vol.%, while the maximum conductivity value was less than 10^{-6} S/cm.

Yoo et al studied segregated systems based on polyphenylene sulfide filled with carbon nanotubes, prepared by mechanical mixing [17]. The values of electrical conductivity ranged from about 10^{-10} S/cm for neat polymer to ~ 0.1 S/cm for 10 wt% of CNT composite, allowing to use these composites as heater elements with regulated maximum heating temperature at 190°C.

Ren et al performed a detailed comparative analysis of the formation of the segregated systems based on UHMWPE filled with boron nitride and with hybrid filler boron nitride-carbon nanotubes [18]. The results of the experiments showed higher thermal conductivity of segregated composites with a hybrid filler, as well as a significant effect of compacting moulding parameters (temperature and pressure) on the thermal properties of the composites.

The most widely used way to prepare the segregated composites is a hot compacting method [19]. On the first stage, the mechanical mixture of polymer powder and filler powder with particle size D and d, respectively, is formed with the condition $D>>d$. In such a way, filler particles cover the surface of polymer particles creating "shell structure". After hot compacting (compression at the temperature of the polymer melting), filler particles remain at boundaries between polymer grains and form a pattern of segregated structure, while the polymer particles conglomerate under pressure creating a solid sample. High electrical conductivity of segregated composites depends widely on processing conditions, in particular rheological properties of polymer matrix which define the segregated structure. High viscosity of melted polymer minimizes the migration of filler particles into polymer grains during hot compacting, reducing the percolation threshold. From this point of view, the ultrahigh molecular weight polyethylene (UHMWPE), having very high viscosity, is a good candidate for the processing of segregated composites [20].

The electrical conductivity of composites with a segregated structure has been studied in many papers [9-15]. However, there is a small number of works devoted to the effect of the filler ordered distribution in the segregated system on the thermal conductivity of CPCs [18]. In this study, the electrical conductivity and thermal conductivity of segregated systems with nano- and microfiller were characterized and these results were discussed comparing them with polymer system in which the filler is statistically distributed. Accordingly, it was investigated the effect of filler particles distribution in the polymer matrix on the electrical and thermal properties of composites from both experimental measurements and modelling on segregated systems filled with carbon nanofiller (graphene), microfiller (anthracite) and hybrid nano-/microfiller.

2. Experimental.

2.1. Materials.

Graphene (Gr) and thermally-treated anthracite (A) were used as fillers. Graphene was produced by Angstron Materials (USA) with following parameters: density 1.89 g/cm^3, specific surface area in the range of 400-800 m^2/g and particle size XY < 10 μm and Z < 3 layers. SEM images of graphene layers are shown in Fig. 1a. Anthracite is a new promising type of carbon filler [21] with the possibility of its modification by an exfoliation and functionalization of the raw material [22]. Recently, the bituminous coals (including anthracite) were proposed as fillers in polymer composites for various applications [23-26]. Raw anthracite with average grain dimensions 0.8 - 1.2 mm was thermally treated in an inert gas (N_2) up to 2000°C to produce a filler with a well-ordered, graphite-like structure (Fig. 1b). The details of a structure and properties of thermally treated anthracite was presented previously by Pusz et al. [21]. Anthracite material, used in this study, has the true density 1.8 g/cm^3 and its particles size was in the range 0.02 to 80 μm, with the largest volume of the fraction in the 4-9 μm range. The thickness of anthracite flakes is mostly below 1 μm.

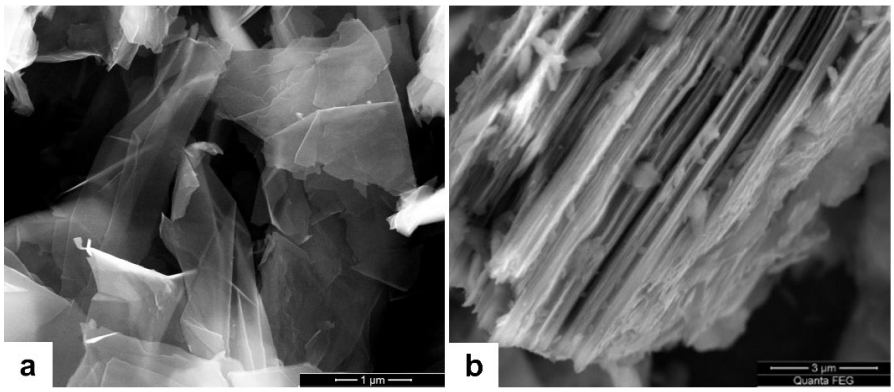

Fig. 1. SEM images of graphene (a) and thermally-treated anthracite (b).

As a polymer matrix for segregated systems, ultra-high molecular weight polyethylene (UHMWPE) Hostalen GUR, type GHR 8110, produced by Hoechst AG (Germany) in a powdered form was chosen. The polymer density is equal to 0.93 g/cm^3 and its melting temperature equal to 137°C. UHMWPE was sequentially sieved through laboratory sieve shaker and the fraction with particle diameters 90-125 μm was used.

Since the molten UHMWPE cannot be extruded due to its high viscosity, for system with a random distribution of filler we used polypropylene (PP) manufactured by Hoechst AG (Germany) with density 0.95 g/cm^3, a melting point at 165°C and melting flow index 7.

2.2. Preparation of composites.

Segregated composites were prepared by the hot compacting method. At the first stage, carbon filler and the polymer particles were thoroughly mixed in a mortar. By this way, the fillers were distributed over the surface of polymer particles creating a coating of carbon layer on the surface of the polymer grains. A uniform mixture of powders of UHMWPE and carbon filler was obtained. At the second stage, the mixture was placed in a steel closed-type mould, heated to 160°C, and compacted within 5 minutes at a pressure of 20 MPa, followed by cooling to room temperature.

A segregated system with a hybrid type of fillers (mixture of two fillers with different shape factors), namely graphene/thermally-treated anthracite (Gr/A) was prepared with a volume filler ratio of Gr/A = 1/3.

For the comparative analysis of the systems with segregated and random filler distribution, the composite PP+A has been prepared by dispersion of the filler in the molten polymer in an originally designed single-screw laboratory extruder with L/D=20 under air atmosphere and temperature of a head-zone of 190°C. To form the samples, the extrudate was ground to particles with a size about 1 mm, which were placed in a mould and pressed during 5 minutes at temperature of 180°C and under a pressure of 20 MPa.

For measuring electrical and thermal conductivities, the samples were prepared in a form of disks with diameter of 30 mm and thickness of 1-1.5 mm.

2.3. Experimental methods.

Microstructure studies were carried out with the Zeiss Primo Star (Carl Zeiss, Germany) optical microscope in a transmission mode on slices with a thickness of 20 μm, cut by a microtome from tested samples.

Characterization of the dielectric permittivity of the samples was determined by means of the broadband dielectric spectroscope ModuLab XM MTS (Solartron Analytical, USA) from 10^6 to 1 Hz at room temperature applying V_{rms} = 5V. The samples with a thickness of 1 mm were placed between two brass electrodes with a diameter of 20 mm.

The DC electrical conductivity σ_{DC} was measured by a two-electrode method. The samples were placed between two steel electrodes with an applied voltage of 10-100 V for conductive and nonconductive samples, respectively. The values of σ_{DC} were estimated from the following equation:

$$\sigma_{DC} = \frac{1}{R} \cdot \frac{h}{S} \qquad (1)$$

where *h* is a thickness of the sample, *R* is electrical resistance measured experimentally using E6-13 teraohmmeter (Radiotechnika, Latvia), and *S* is a sample area.

Transient plane source method [27] was applied to measure thermal conductivity of the composites at room temperature using the TPS 2200S (HotDisk AB, Sweden) with a sensor that was located between two same tested samples [28, 29]. All experiments were carried out in "Standard Analysis" mode, which follows the standard ISO 22007-2 (Plastics -- Determination of thermal conductivity and thermal diffusivity -- Part 2: Transient plane heat source (hot disc) method).

Melting and crystallization temperatures were determined by differential scanning calorimetry using Q2000 (TA Instruments, USA) with a heating/cooling rate of 20°C/min.

Density was measured by hydrostatic method (ISO 6783:1982) using Mettler Toledo's Density Kits.

3. Results and discussion.

3.1. Morphology of the composites.

The results of electron and optical microscopy of the systems with segregated distribution of the filler are shown in Fig. 2.

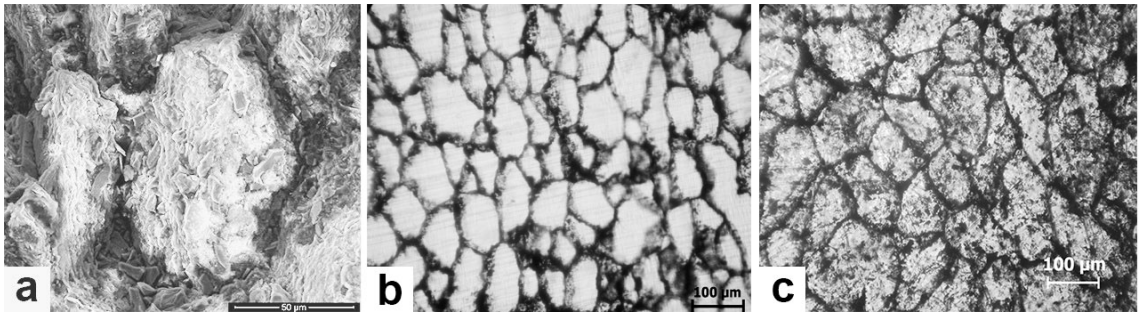

Fig. 2. Scanning electron microscopy (a) and optical microscopy (b, c) images of segregated UHMWPE based composites filled with anthracite: a, c – segregated UHMWPE+A structure with 3 vol.% and b – with 1 vol.% of filler.

In segregated system the filler particles are localized at the boundaries between the polymer grains, one can see the separate particles of anthracite located between polymer granules (Fig. 2a). With a small filler content, the filler particles localized in the intergrain boundaries do not create the conductive network (Fig. 2b). With the increase in the filler concentration, the walls of the framework become thicker, forming a continuous conductive phase in the composite (Fig. 2c).

3.2. Electrical conductivity of composites.

The results of the electrical conductivity σ_{DC} of the composites studied as function of volume content of the fillers φ are shown in Fig. 3. The electrical conductivity of all systems demonstrates percolation behaviour with a sharp increasing by 10 orders of magnitude when the percolation threshold φ_c is reached.

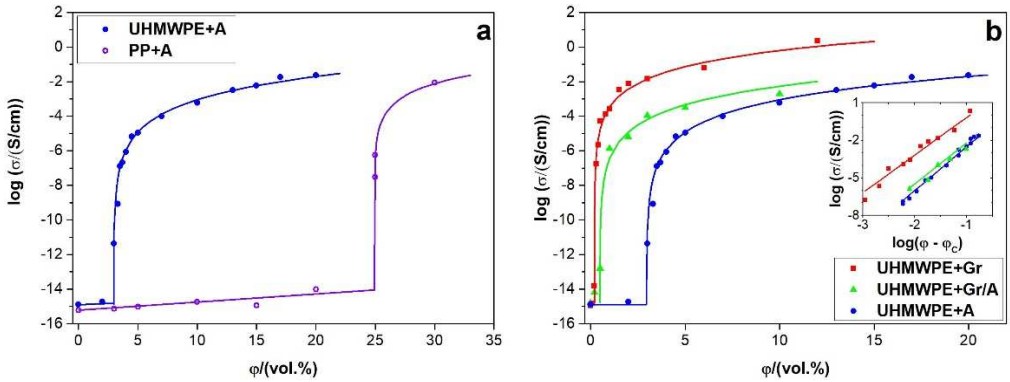

Fig. 3. a - Dependence of electrical conductivity versus concentration for systems with segregated structure of UHMWPE+A and with random distribution of filler PP+A; b - Comparison of concentration dependencies of electrical conductivity for segregated systems filled with monofillers (microfiller A and nanofiller Gr) and hybrid filler (Gr/A).

The behaviour of the electrical conductivity of systems above the percolation threshold is described by the well-known percolation equation [30, 31]:

$$\sigma = \sigma_0 \cdot (\varphi - \varphi_c)^t \qquad (2)$$

where φ is the volume fraction of the filler, φ_c is the percolation threshold of the system, σ_0 is the adjustable parameter, determined by the electrical conductivity of the filler, and t is the critical exponent. Using Eq. (2) in the logarithmic form, the last two parameters of the model were determined by fitting the experimental results of electrical conductivity of the systems using the Eq. (3):

$$\log\sigma = \log\sigma_0 + t \cdot \log(\varphi - \varphi_c) \qquad (3)$$

In the coordinates log σ ~ log (φ - φ_c) the percolation curves become linear and enable to define the parameters t and σ_0 of Eq. (2). Example of the fitting illustrated in the insertion of Fig. 3b. Percolation parameters of all tested systems are given in Table 1.

Table 1. Percolation parameters of Eq. (2) and (6).

Composite	Type of structure	$\varphi_c < \varphi$		$\varphi_c > \varphi$	
		φ_c/(vol.%)	t	φ_c/(vol.%)	-s
PP+A	random	24.8	2.4	25.5	0.73
UHMWPE+A	segregated	2.95	3.5	3.8	0.88
UHMWPE+Gr	segregated	0.21	3.0	0.3	0.85
UHMWPE+Gr/A	segregated	0.49	3.3	0.5	0.85

Fig. 3a shows a significant difference in the conductivity behaviour of systems with a homogeneous particle distribution (PP+A) and a segregated structure (UHMWPE+A). The data in Table 1 give the percolation threshold value which is an order of magnitude higher for the system with random filler distribution compared with the segregated composite. This effect originates by the segregated structure of the composite, in which the filler is located on the boundaries between the polymer grains (see Fig. 2). Such morphology leads to the formation of a conducting framework in which the local concentration of the filler φ_{loc} is much higher than the average concentration, φ, related to the entire volume of the sample, $\varphi_{loc} > \varphi$ [10, 32].

The critical exponent t of the segregated system exceeds the theoretical value $t \approx 2$ [33]. High value can be explained by the evolution of the conductive phases morphology, the shape of the filler particles, its non-statistical distribution, and the appearance of aggregates. Also, the values of t can be affected by the interaction of filler particles with the polymer, contact resistance between them [34, 35].

Fig. 3b shows the comparative results of the electrical conductivity of segregated systems based on UHMWPE filled with microfiller A, nanofiller Gr and hybrid filler Gr/A with a volumetric ratio of Gr/A = 1/3. The lowest percolation threshold is equal to 0.21 vol.% for the system with nanofiller Gr, while it reaches 2.95 vol.% in the system with microfiller A.

In composites with hybrid filler (micro and nano fillers), the percolation threshold is 0.49 vol.%, while the calculated value obtained by the mixture rule (taking for calculation $\varphi_{c(Gr)}$ = 0.21 vol.% and $\varphi_{c(A)}$ = 2.95 vol.% with their volumetric ratio 1/3) is 2.3 vol.%. Such strong decrease in the experimental value of the percolation threshold, as compared to the calculated value, is a consequence of the synergetic effect of a combination of nano- and microfiller. This synergism can be explained by the bridging effect, in which the nanofiller particles with high shape factor are distributed in the interstices between the microparticles. The nanofillers help to bridge microfillers making local contacts and developing percolation cluster, thus

ensuring charge transport at lower filler concentration. Similar synergetic effects were also obtained in previous studies by mixing carbon nanofillers such as graphene, nanotubes and carbon black nanoparticles [36-38].

Deplancke et al [39] propose to estimate the thickness e of the filler layer on the intergrain boundary of segregated system at a concentration of filler corresponding to the percolation threshold, $\varphi = \varphi_c$, as

$$e = R - \left[R^3 \left(1 - \frac{\varphi_c}{\varphi_{cr}} \right) \right]^{\frac{1}{3}} \qquad (4)$$

where R is the radius of a polymer particle, φ_c is the value of percolation threshold in the segregated system, φ_{cr} is the value of percolation threshold for a homogeneous (random) distribution of filler in the polymer matrix (symbols in Eq. (4) taken from [39] are replaced with those used in this work). Previously, the models of the segregated filler structure were proposed [10, 32], in which thickness of the framework walls created by filler was defined as nd, where n is the number of filler monolayers in the framework wall, d is the particle size of filler. Obviously, $e = nd$. The geometric model of the segregated system [10] (as well as the computer simulations [32]) suggests that percolation occurs at a wall thickness of at least one layer. This means that the polymer particles are covered only partially with a layer of the filler particles and when compacted they are combined into a single-layer wall of the framework. This case is described in [40]. From the equations given in [10, 32], the thickness of the wall of segregated framework can be estimated by the following equation:

$$e = nd = D \left[1 - \left(1 - \frac{\varphi_c}{\varphi_{cr}} \right)^{\frac{1}{3}} \right] \qquad (5)$$

where D=2R is a diameter of the filler particle (i.e. period of the framework in the models [10, 32]).

For the segregated UHMWPE+A systems containing anthracite, the values of D and d are 100 μm and 5 μm, respectively. The values of φ_c for UHMWPE+A and φ_{cr} PP+A composites are taken from the Table 1. Calculation of the layer thickness e of the segregated filler using Equations (4) and (5) gives 2.07 μm and 4.14 μm, respectively. The value e = 4.14 μm means the thickness of the framework wall close to one layer ($n \approx 1$) of the filler whereas Eq. (4) gives twice smaller thickness of the wall (i.e. half of layer), which seems to be

underestimated. Geometrical details of the UHMWPE+A electron microscopic image (Fig. 2a) are in agreement with the calculation by Eq. (5).

3.3. Dielectric permittivity of composites.

The dependence of the dielectric permittivity of the composites versus volume filler content in the region $\varphi < \varphi_c$ is plotted in Fig. 4. As shown, the values of permittivity ε_r sharply increase by increasing concentration of conductive filler. The difference between composites with random (PP+A) and segregated (UHMWPE+A) distribution of the filler can be explained by formation of the conductive cluster at lower concentrations in the framework of the segregated structure.

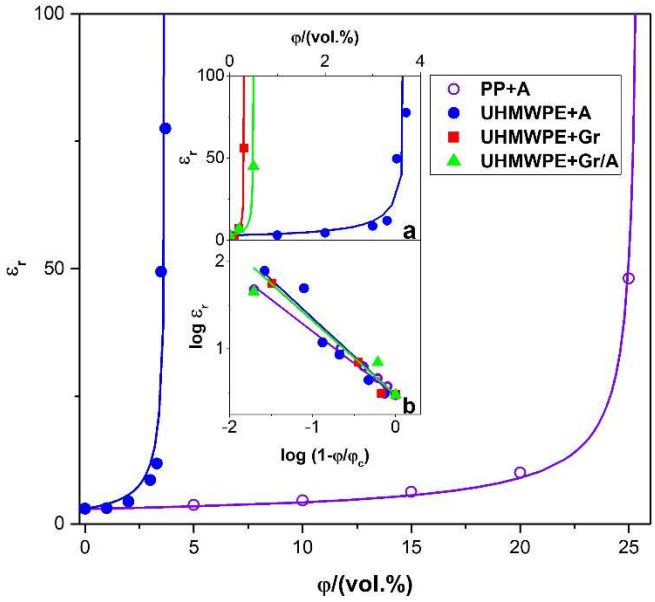

Fig. 4. Dielectric permittivity of the systems with segregated structure (UHMWPE+A) and with random distribution of filler (PP+A) as a function of filler content. Inserts show dielectric permittivity of the segregated systems (upper) and fitting of percolation curves in double logarithmic scale (lower). Points are the experimental data at 1 kHz, lines are the calculated values with accordance of Eq. (4).

Since permittivity behaviour has a percolation nature, the experimental points can be described by the percolation model [31, 41]:

$$\varepsilon_r = \varepsilon_m \left(\frac{\varphi_c - \varphi}{\varphi_c} \right)^{-s} \qquad (6)$$

Where ε_r and ε_m are permittivity of composite and matrix, respectively, φ is the volume fraction of the filler, φ_c is the percolation threshold of the system, and s is dielectric critical exponent. Parameters ε_m and s are adjustable and can be obtained from the fitting Eq. (7) to the experimental data in the log ~ log scale.

$$\log \varepsilon_r = \log \varepsilon_m - s \log\left(\frac{\varphi_c - \varphi}{\varphi_c}\right) \qquad (7)$$

Log-log plots of the fitting are illustrated in Fig. 4b and parameters are given in the Table 1. Fitted percolation curves are in good agreement with experimental points and illustrated in the Fig. 4 and 4a (the colours of the lines correspond to the colours of the symbols). The data in the Table 1 show that dielectric percolation thresholds correspond to the values of φ_c for electrical percolation thresholds. Theoretical value of dielectric critical exponent for system with random filler distribution is equal to 0.7-0.75 [41, 42]. As shown in Table 1, the values of s are in good agreement with the theoretical values for the composite with a random distribution of the filler PP+A. For segregated systems, the values of the critical exponent are exceeded, the values of s are in the range 0.85-0.88. The same effect was observed for the critical index t in the region above the percolation threshold, the values of t for segregated composites exceed the values for the PP+A system with a random distribution of the filler. Thus, the non-statistical distribution of the filler deviates the critical exponents from the universal values.

3.4. Thermal properties.

3.4.1. Modelling of thermal conductivity.

Generally, the dependence of the thermal conductivity (TC) of two-phase polymer-filler systems versus filler concentration lie within the area limited by Wiener bounds [43, 44], upper bound and lower bound. The Wiener bounds constitute two extreme cases of the effective conductivity, namely, in series or in parallel morphological structure of two phase system with conductivities λ_1 and λ_2 ($\lambda_2 >> \lambda_1$). The conductivity of parallel or series structure of two phase system, corresponding to upper and lower Wiener bounds, is described by the following equations, respectively:

$$\lambda = (1 - \varphi)\lambda_1 + \varphi\lambda_2 \qquad (8)$$

$$\lambda = \left(\frac{1-\varphi}{\lambda_1} + \frac{\varphi}{\lambda_2}\right)^{-1} \qquad (9)$$

Fig. 5a shows a parallel structure in which the conductivity is determined by the content of the high-conductive component λ_2 (upper bound) while in the series structure (Fig. 5b), the total conductivity is determined by the conductivity of the low-conductive component λ_1 (lower bound). In the case of the structure of a continuous matrix having λ_1 and inclusions with λ_2 (Fig. 5c), the total conductivity depends on the conductivity of both phases, as well as the size, the shape, the spatial distribution of inclusions in the matrix, and the interactions between phases.

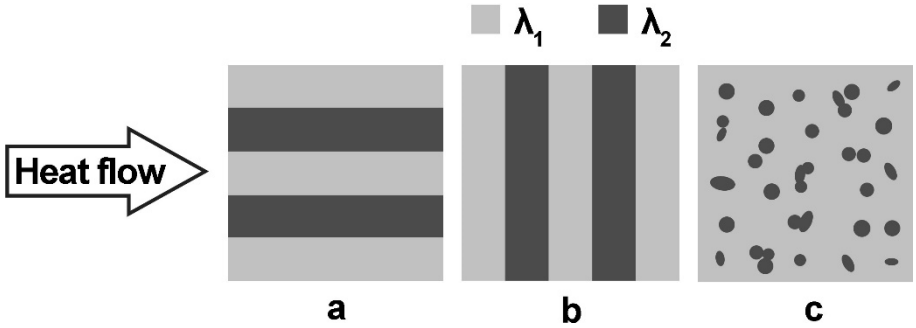

Fig. 5. Parallel structure (a), series structure (b) and dispersed distribution of phase 2 in the continuous phase 1 (c). Phase conductivities are denoted by λ_1 and λ_2.

It was found elsewhere [10] that the Lichtenecker model [45] (also known as geometric mean model) corresponds well to the experimental data of particulate polymer composites. The Lichtenecker equation is given below:

$$\lambda = \lambda_1^{1-\varphi} \cdot \lambda_2^{\varphi} \qquad (10)$$

also in logarithmic form:

$$\log \lambda = (1-\varphi)\log \lambda_1 + \varphi \log \lambda_2 \qquad (11)$$

Theoretical concentration dependence of the thermal conductivity, calculated according to the Eq. (8) - (11) for the two-phase system with fixed thermal conductivity values λ_1 = 0.1 W/m·K and λ_2 = 100 W/m·K is shown in Fig. 6 in logarithmic scale. In latter case, the Lichtenecker Eq. (11) is depicted by linear dependence since it is a case of mixture depicted by Eq. (10) for logarithmic conductivities. The curves corresponding to the Wiener bounds (the parallel and series models) create antisymmetric position relatively to the line of Eq. (11).

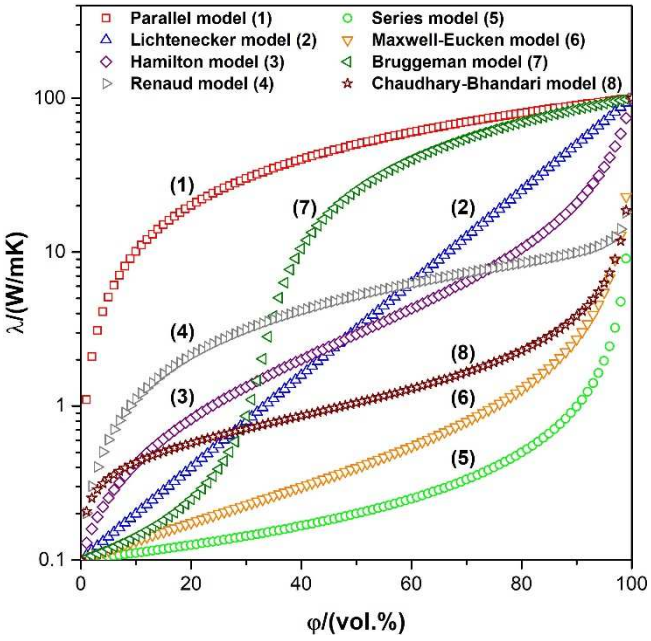

Fig. 6. Predictions of the thermal conductivity of the two-phase system at fixed values of λ_1 = 0.1 W/m·K, λ_2 = 100 W/m·K and of model parameters f = 0.1 (Renaud model), f = 0.3 (Chaudhary-Bhandari model), k = 30 (Hamilton model) as a function of volume fraction of the dispersed phase.

A number of models suggest the description of TC by various combinations of the parallel and series case, for example Renaud, Krischer and Chaudhary–Bhandari models, respectively [46]:

$$\lambda = f\left((1-\varphi)\lambda_1 + \varphi\lambda_2\right) + (1-f)\left(\frac{1-\varphi}{\lambda_1} + \frac{\varphi}{\lambda_2}\right)^{-1} \qquad (12)$$

$$\lambda = \left(\frac{1-f}{(1-\varphi)\lambda_1 + \varphi\lambda_2} + f\left(\frac{1-\varphi}{\lambda_1} + \frac{\varphi}{\lambda_2}\right)\right)^{-1} \qquad (13)$$

$$\lambda = \left((1-\varphi)\lambda_1 + \varphi\lambda_2\right)^{f}\left(\frac{1-\varphi}{\lambda_1} + \frac{\varphi}{\lambda_2}\right)^{(f-1)} \qquad (14)$$

where f is an adjustable parameter, $0 \le f \le 1$ indicating the contribution of the parallel and series structures.

The expression for TC of suspension of the spherical non-contacting particles was derived by Maxwell, it usually used in the modified form and is known as Maxwell-Eucken equations [47, 48]:

$$\lambda = \lambda_1 \frac{2\lambda_1 + \lambda_2 + 2\varphi(\lambda_2 - \lambda_1)}{2\lambda_1 + \lambda_2 - \varphi(\lambda_2 - \lambda_1)} \qquad (15)$$

The Maxwell equation is well satisfied only with a small content of the dispersed phase and gives underestimated values of TC at higher concentrations. One of the modifications to the Maxwell model is the Hamilton equation, which includes the adjustable *k* parameter, so that it becomes more "flexible" [46]:

$$\lambda = \lambda_1 \frac{(k-1)\lambda_1 + \lambda_2 - (k-1)(\lambda_1 - \lambda_2)\varphi}{(k-1)\lambda_1 + \lambda_2 + (\lambda_1 - \lambda_2)\varphi} \qquad (16)$$

The widely known Bruggeman model uses the effective medium approximation (EMA) and has no limitations for the concentration of inclusions [47, 49]:

$$(1-\varphi)\frac{\lambda - \lambda_1}{2\lambda + \lambda_1} + \varphi\frac{\lambda - \lambda_2}{2\lambda + \lambda_2} = 0 \qquad (17)$$

This model can be used for concentrated suspensions, where a particle clustering effect is observed. At low concentrations of a filler (less than 30 vol.%), the thermal conductivity depends essentially on the matrix conductivity, while at high filler loading (above 40-50 vol.%), the TC of composite approaches to the conductivity of filler particles. As shown in [47], the Bruggeman equation has a characteristic shape with a like-percolation behaviour in the region of 30-40 vol.% of dispersed inclusions. Calculations performed according to the above formulas are shown in Fig. 6.

All these equations and many others lie within the Wiener bounds and describe different types of particulate composites depending on properties of the filler and the matrix, the content of filler, its anisotropy, its orientation, its dispersion and so on [50, 51].

3.4.2. Experimental results.

The results of measurements of the thermal conductivity of composites in logarithmic scale are shown in Fig. 7. As it can be seen from the figure, all the thermal conductivity curves versus filler content are well described by the Lichteneker equation. In our case, based on the Eq. (10), $\lambda_1=\lambda_p$, $\lambda_2=\lambda_f$, then Eq. (11) takes the form:

$$\log\lambda = (1-\varphi)\log\lambda_p + \varphi\log\lambda_f \qquad (18)$$

where λ_p is the TC of the polymer matrix, λ_f is the TC of the filler.

In many works [10, 52, 53], it was shown that the Lichtenecker model and the modified Lichtenecker model (the Agari-Uno model) describe the thermal conductivity of polymer-dispersed filler systems in the best way. However, for other systems, different models can give better results [46]. In our case, the Lichtenecker model gives the most adequate correspondence between the experimental and calculated values.

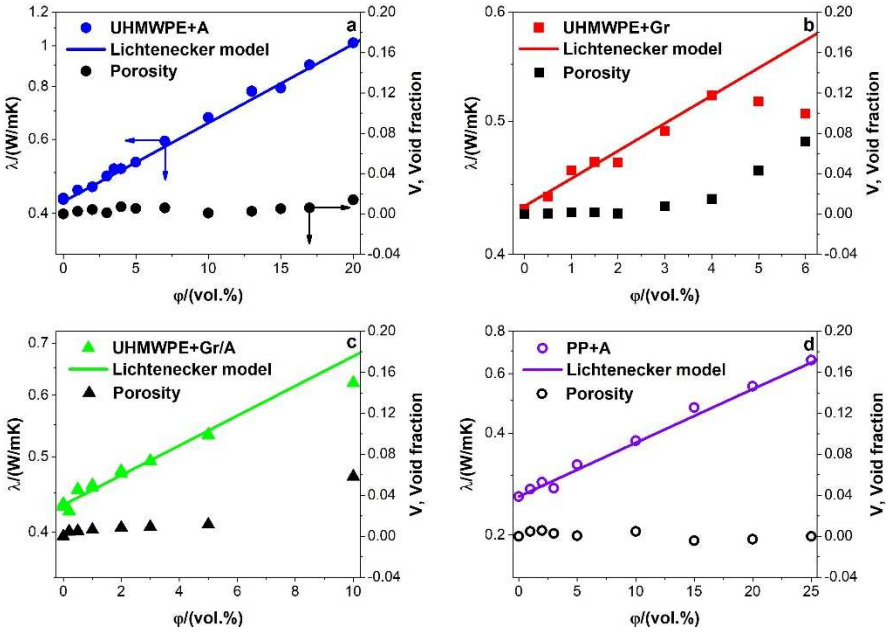

Fig. 7. Thermal conductivity of the composites with segregated distribution of the filler (a-c) and random distribution (d), points – experimental values, solid lines – calculation in accordance with Eq. (18). The plots also show the porosity of the composites calculated by Eq. (19).

For composites with the microfiller, UHMWPE+A and PP+A, the Lichtenecker model and experimental data are consistent across the entire filler content, whereas in composites with graphene and hybrid filler at filler contents exceeding 4 vol.% and 10 vol.% respectively, the experimental TC values decrease in comparison with the theoretical ones. The reason of such effect can be the formation of non-wetted aggregates of nanofiller particles at a high content of filler in the composite. This is confirmed by the correlation between the decrease in thermal conductivity and the decrease in the density of the composites, since the appearance of non-wetted (porous) aggregates in the system leads to a decrease in the density of the composite. To evaluate the non-wetted volume of composites, the Eq. (19) was used:

$$V = \frac{\rho_{theor} - \rho_{\exp}}{\rho_{theor}} \qquad (19)$$

where ρ_{theor} – theoretical values of the composites density calculated by mixture rule ($\rho_{theor} = \varphi \cdot \rho_{filler} + (1-\varphi) \cdot \rho_{pol}$) and ρ_{exp} – experimental values obtained by hydrostatic method. The results of the calculations were plotted in Figure7.

Microfiller does not create unwetted aggregates, even at high content in the composite (figures 7a and 7d). The correspondence between the changes in TC and the density of the composites was also observed in [10] for metal-filled systems.

Table 2. Thermal parameters of composites

Composite	Type of structure	λ_p / (W/m·K)	λ_f / (W/m·K)	T_m / (°C)	T_c / (°C)	$\Delta T=T_m-T_c$ / (°C)
PP+A	random	0.26	7.2	-	-	-
UHMWPE+A	segregated	0.43	31.6	137	106	31
UHMWPE+Gr	segregated	0.43	44.7	137	104	33
UHMWPE+Gr/A	segregated	0.43	35.5	137	107	30

* For pure UHMWPE T_m=137 °C, T_c=112 °C, ΔT=25 °C

A good agreement between the experimental values of TC and the theoretical values calculated according to Eq. (18) is observed and values used for the model are listed in Table 2. It should be noted that the λ_2 values in Eq. (8) - (17) correspond to the bulk thermal conductivity of the high-conductive phase. In our case, λ_f is the thermal conductivity of the dispersed filler and has much lower values than its bulk thermal conductivity. For graphite, for example, the TC given in the literature is around λ_2 = 100-400 W/m·K [54]. Similar results were obtained for the segregated PVC+CNT system [52]. This is due to the fact that the thermal conductivity of the dispersed phase λ_f depends on the interfacial thermal resistance (also known as Kapitza resistance), which includes the thermal resistance of the particle-particle contact and the interfacial thermal resistance between the particle and the polymer matrix. Both components limit the transport of heat flow through the disperse filler phase.

The obtained value of λ_f for segregated systems are much higher than for PP+A composite with a random filler distribution, namely 31.6 W/m·K versus 7.2 W/m·K, i.e. λ_f for segregated system is 4.4 times higher. The higher thermal conductivity of the conductive phase in the segregated structure indicates a better thermal transport through the filler phase. This result is obviously associated with a high local concentration of the filler in the intergrain polymer layer compared to a low average concentration with a random distribution of the filler throughout the polymer matrix.

The hybrid Gr/A filler has shown a synergistic effect with respect to the percolation threshold of electrical conductivity, which is much lower in the UHMWPE+Gr/A composite than the percolation threshold calculated by the rule of the mixture (see section 3.2). The calculation of λ_f for systems with hybrid filler by the rule of the mixture for composites UHMWPE+Gr and UHMWPE+A taken in the ratio 1/3 gives a value of 34.9 W/m·K, which is close to the

experimental value λ_f = 35.5 W/m·K for the UHMWPE+Gr/A composite with hybrid filler. Hence, in the case of thermal conductivity, unlike electrical conductivity, no synergistic effect is observed. These differences seem to be due to the fact that the electrical conductivity is provided exclusively by the filler, and the polymer matrix is an insulator, whereas in the transport of heat flow both phases, the polymer phase and the filler phase, take part. In this case the effect of changes in the structure of the dispersed phase is not determining.

Huxtable et al found that experimental thermal conductivity of polymer-CNT composites is significantly lower than that calculated one when, as λ_2, the intrinsic conductivity of nanotubes was taken, since the heat flux is limited by low interfacial thermal conductivity [55]. They have shown that the effective thermal resistance between two nanotubes is always equal/greater than the equivalent thermal resistance of a polymer layer of 40 nm thick. Different studies including the previous one allowed Hida et al to conclude that the thermal conductivity of the composite is controlled mainly by interfacial thermal conductivity caused by phonon scattering at the interphase boundaries [56]. Indeed, in refs. [57-60], the thermal conductivity of polymer systems containing high-conductive filler BN (λ_{BN} = 250 W/m K) was in the range of 0.7–1.1 W/m K with a maximum BN content up to 60 wt.%.

The same reason can explain the absence of a percolation threshold on the concentration dependences of thermal conductivity. Calculation of thermal resistance R_{con} of contact spots between metal particles and polymer interlayer between filler particles was developed in particular by Mamunya et al [61]. They showed that the R_{con} of a contact spot is two orders of magnitude higher than the R_{pl} of polymer layer filling the space between the contacting particles. It follows that formation of conducting clusters due to contacting filler particles at percolation will not contribute to thermal conductivity of a composite, although it will provide the appearance of electrical conductivity. Shenogina et al. noted that a high value of interfacial thermal resistance suppresses the heat flux through the conducting CNT network with an increase of filler content in a composite that leads to the absence of percolation behaviour [62].

3.5. Thermal properties.

The thermal properties of segregated composites with different concentrations of micro- and nanofillers have been studied by the DSC method. Fig. 8 shows the results of measurements in the second heating cycle (determination of the melting point T_m) and in the first cooling cycle (determination of the crystallization temperature T_c). As shown, the melting point does not depend on content of the filler (with scattering in the range of ±2°C). This seems obvious,

since the filler is located only in the intergrain layer of the polymer matrix and the bulk of the polymer is free of filler, consequently, its influence is minimal. A similar dependence of T_m on the filler content was also observed in [39] for the segregated UHMWPE system with nanotubes.

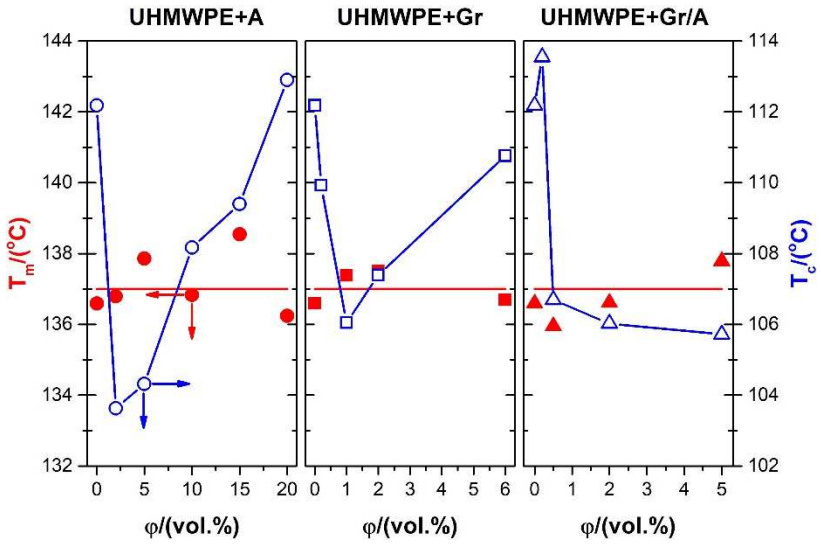

Fig. 8. Concentration dependence of melting point temperature T_m (left axis, filled symbols) and crystallization temperature T_c (right axis, blank symbols) in segregated systems.

However, it is possible to observe the influence of the filler on the crystallization temperature of polyethylene, which is surprising, taking into account the foregoing consideration of the segregated structure of the composites. With a minimum filler content (1 vol.% for Gr, 2 vol.% for A and 0.5 vol.% for Gr/A), the crystallization temperature T_c is reduced (data are given in Table 2). The supercooling temperature $\Delta T = T_m - T_c$ increases from 25 °C for pure polymer to 33-30 °C for composites with a minimum filler content. An increase in ΔT indicates inhibition of crystallization process of polyethylene in the presence of filler particles. Hence, the influence of the surface of the filler particles located in the intergrain layers on the process of structure formation in the polymer matrix extends to the zone of the pure polymer.

With increasing filler content in UHMWPE+A and UHMWPE+Gr systems, the crystallization temperature begins to increase and reaches the value typical for the unfilled polymer. It follows that the filler particles at its high concentration can serve as centres of crystallization and increase T_c. However, in the case of hybrid filler this effect is absent, the

value of T_c is almost unchanged, apparently the hybrid particles are more interconnected and do not penetrate into the volume of polymer granules as their concentration increases.

4. Conclusions.

Formation of the segregated structure, in which the filler particles are localized on the surface of the polymer grains, leads to the formation of the conductive framework in the polymer matrix and significantly reduces the electrical percolation threshold of the systems.

It was shown that, in the case of electrical conductivity, the value of the percolation threshold in the segregated system UHMWPE+A is one order of magnitude lower than at the composite with random distribution of filler PP+A. For segregated system filled with nanofiller graphene (UHMWPE+Gr), the percolation threshold is much lower than that for the system with microfiller anthracite (UHMWPE+A). The hybrid filler graphene/anthracite (Gr/A), exhibits a percolation threshold far below than the value calculated using rule mixture. Synergism of the hybrid micro/nanofiller is explained by the bridging effect, which is caused by the arrangement of nanoparticles between microparticles of the filler.

Experimental results of thermal conductivity for all systems do not reveal the percolation behaviour and can be well described by the Lichtenecker model. Deviations from the model at high filler concentrations are associated with the formation of unwetted aggregates and correlate with the change in the density of the composites.

Thermal conductivity of the composites can be characterized by the parameter λ_f, which is the thermal conductivity of the dispersed filler including the interfacial thermal resistance. It was shown that the value of λ_f for segregated systems is 4.4 times higher than that for a composite with random distribution of the filler particles. This result proves that the thermal transport through the filler phase in the segregated structure is increased, which is obviously associated with a high local concentration of the filler in the framework walls, compared to low average filler concentration in the composite with random distribution of the filler particles throughout the polymer matrix.

The melting point T_m of all segregated composites remains constant independently on the filler content, whereas the crystallization temperature T_c is linked with the content of the filler. At low filler content, T_c decreases, which leads to an increase in the supercooling temperature and indicates a retardation of the crystallization in the presence of the filler. The subsequent

increase in T_c upon further filling may be due to the growth of crystallization centres with higher filler content.

Acknowledgements

Oleksii Maruzhenko acknowledges the French embassy in Ukraine and Ecole Doctorale for supporting project № 872239L.

This work was partially realized in the frame of Polish-Ukrainian (PAS-NASU) joint project "Development of modern polymer nanocomposites with various graphene-like carbon nanofillers".

References

[1] S. Yellampalli (Ed), Carbon nanotubes – polymer nanocomposites, InTech, Croatia, 2011.

[2] K. Friedrich, U. Breuer, Multifunctionality of polymer composites. Challenges and new solutions, Elsevier Inc., USA, 2015.

[3] J. Du, H.M. Cheng, The fabrication, properties, and uses of graphene/polymer composites, Macromol Chem Phys 213(10-11) (2012) 1060-1077.

[4] J. Cuppoletti (Ed), Metal, ceramic and polymeric composites for various uses, InTech, Croatia, 2011.

[5] M. Naveen, N. Gurudatt, Y. Shim, Applications of conducting polymer composites to electrochemical sensors: A review, Appl Mater Today 9 (2017) 419-433.

[6] K. Nasouri, A. Shoushtari, Designing, modeling and manufacturing of lightweight carbon nanotubes/polymer composite nanofibers for electromagnetic interference shielding application, Compos Sci Technol 145 (2017) 46-54.

[7] F. Wang, L. Drzal, Y. Qin, Z. Huang, Processing and characterization of high content multilayer graphene/epoxy composites with high electrical conductivity, Polym Compos 37 (2016) 2897-2906.

[8] D. Li, Q. Chen, Y. Yang, Y. Chen, C. Xiao, Effects of flake graphite on property optimisation in thermal conductive composites based on polyamide 66, Plast Rubber Compos 46(6) (2017) 266-276.

[9] R.P. Kusy, Applications, in: S.K. Bhattacharya (Ed.), Metal-filled polymers, Marcel Dekker, New York, 1986, pp.1-142

[10] Ye.P. Mamunya, V.V. Davidenko, P. Pissis, E.V. Lebedev, Electrical and thermal conductivity of polymers filled with metal powders, Europ Pol J 38 (2002) 1887-1897.

[11] H. Pang L. Xu, D. Yan, Z. Li, Conductive polymer composites with segregated structures, Prog Polym Sci 39(11) (2014) 1908-1933.

[12] Ye.P. Mamunya, N. Lebovka, M. Lisunova, E. Lebedev, A. Rybak, G. Boiteux, Conductive polymer composites with ultralow percolation threshold containing carbon nanotubes, J Nanostruct Polym Nanocompos 4 (2008) 21-27.

[13] A. Mierczynska, M. Mayne-L'Hermite, G. Boiteux, J.K. Jeszka, Electrical and mechanical properties of carbon nanotube/ultrahigh-molecular-weight polyethylene composites prepared by a filler prelocalization method, J Appl Polym Sci 105 (2007) 158-168.

[14] T. Gong, S. Peng, R. Bao, W. Yang, B. Xie, M. Yang, Low percolation threshold and balanced electrical and mechanical performances in polypropylene/carbon black composites with a continuous segregated structure, Compos Part B-Eng 99 (2016) 348-357.

[15] Ye.P. Mamunya, V.V. Levchenko, A. Rybak, G. Boiteux, E.V. Lebedev, J. Ulanski, G. Seytre, Electrical and thermomechanical properties of segregated nanocomposites based on PVC and multiwalled carbon nanotubes, J Non-Cryst Solids 356(11-17) (2010) 635-641.

[16] N. George, P. Bipinbal, B. Bhadran, A. Mathiazhagan, R. Joseph, Segregated network formation of multiwalled carbon nanotubes in natural rubber through surfactant assisted latex compounding: A novel technique for multifunctional properties, Polymer 112 (2017) 264-277.

[17] T.J. Yoo, E.B. Hwang, Y.G. Jeong, Thermal and electrical properties of poly(phenylene sulfide)/carbon nanotube nanocomposite films with a segregated structure, Compos Part A Appl Sci Manuf 91 (2016) 77-84.

[18] P. Ren, S. Hou, F. Ren, Z. Zhang, Z. Sun, L. Xu, The influence of compression molding techniques on thermal conductivity of UHMWPE/BN and UHMWPE/(BN+MWCNT) hybrid composites with segregated structure, Compos Part A Appl Sci Manuf 90 (2016) 13-21.

[19] Y. Mamunya, Carbon nanotubes as conductive filler in segregated polymer composites – electrical properties, in: S. Yellampalli (Ed.), Carbon nanotubes – polymer nanocomposites, InTech, Croatia, 2011, pp. 173-196.

[20] C. Zhang, C. Ma, P. Wang, M. Sumita, Temperature dependence of electrical resistivity for carbon black filled ultra-high molecular weight polyethylene composites prepared by hot compaction, Carbon 43 (2005) 2544-2553.

[21] S. Pusz, U. Szeluga, B. Nagel, S. Czajkowska, H. Galina, J. Strzezik, The influence of structural order of anthracite fillers on the curing behavior, morphology, and dynamic mechanical thermal properties of epoxy composites, Polym Compos 36 (2014) 336-247.

[22] B. Kumanek, U. Szeluga, S. Pusz, A.F. Borowski, P.S. Wrobel, A. Bachmatiuk, J. Kubacki, M. Musioł, O. Maruzhenko, B. Trzebicka, Multi-layered graphenic structures as the effect of chemical modification of thermally treated anthracite, Fuller Nanotub Car N 26(7) (2018) 405-416.

[23] B.D. Keller, N. Ferralis, J.C. Grossman, Rethinking coal: thin films of solution processed natural carbon nanoparticles for electronic devices, Nano Lett. 16 (2016) 2951-2957.

[24] S. Li, X. Li, Q. Deng, D. Li, Three kinds of charcoal powder reinforced ultra-high molecular weight polyethylene composites with excellent mechanical and electrical properties, Mater. Des. 85 (2015) 54-59.

[25] X.H. Meng, Y.H. Zhang, J.B. Lu, Z.L. Zhang, L.P. Liu, et al., Effect of bamboo charcoal powder on the curing characteristics, mechanical properties, and thermal properties of styrene-butadiene rubber with bamboo charcoal powder, J. Appl. Polym. Sci. 130 (6) (2013) 4534-4541.

[26] S. Belaïd, G. Boiteux, P. Cassagnau, Rheological and electrical properties of EVA copolymer filled with bamboo charcoal, Rheol. Acta 52 (1) (2013) 75-84.

[27] X. Yang, C. Liang, T. Ma, Y. Guo, J. Kong, J. Gu, M. Chen, J. Zhu, A review on thermally conductive polymeric composites: classification, measurement, model and equations, mechanism and fabrication methods, Adv Compos Hybrid Mater 1(2) (2018) 207-230.

[28] S.E. Gustafsson, Transient plane source techniques for thermal conductivity and thermal diffusivity measurements of solid materials, Rev Sci Instrum 62(3) (1991) 797-804.

[29] V. Bohac, M. Gustavsson, L. Kubicar, S. Gustafsson, Parameter estimations for measurements of thermal transport properties with the hot disk thermal constants analyser, Rev Sci Instrum 71(6) (2000) 2452-2455.

[30] S. Kirkpatrick, Percolation and Conduction, Rev Mod Phys 45(4) (1973) 574-588.

[31] D. Stauffer, A. Aharony, Introduction to Percolation Theory, CRC press, London, 1994.

[32] N. Lebovka, M. Lisunova, Y. Mamunya, N. Vygornitskii, Scaling in percolation behaviour in conductive–insulating composites with particles of different size, J Phys D Appl Phys 39(10) (2006) 2264-2271.

[33] M.D. Rintoul, S. Torquato, Precise determination of the critical threshold and exponents in a three-dimensional continuum percolation model, J Phys A-Math Gen 30(16) (1997) L585.

[34] E.P. Mamunya, V.V. Davidenko, E.V. Lebedev, Percolation conductivity of polymer composites filled with dispersed conductive filler, Polym Compos 16(4) (1995) 319-324.

[35] E.P. Mamunya, V.V. Davidenko, E.V. Lebedev, Effect of polymer-filler interactions on percolation conductivity of thermoplastics filled with carbon black, Compos Interface 4(4) (1997) 169-176.

[36] P.C. Ma, M.Y. Liu, H. Zhang, S.Q. Wang, R. Wang, K. Wang, Y.K. Wong, B.Z. Tang, S.H. Hong, K.W. Paik, J.K. Kim, Enhanced electrical conductivity of nanocomposites containing hybrid fillers of carbon nanotubes and carbon black, ACS Appl Mater Interfaces 1(5) (2009) 1090-1096.

[37] M.H. Al-Saleh, Electrical and mechanical properties of graphene/carbon nanotube hybrid nanocomposites, Synth Met 209 (2015) 41-46.

[38] U. Szeluga, B. Kumanek, B. Trzebicka, Synergy in hybrid polymer/nanocarbon composites. A review, Compos Part A Appl Sci Manuf 73 (2015) 204-231.

[39] T. Deplancke, O. Lame, S. Barrau, K. Ravi, F. Dalmas, Impact of carbon nanotube prelocalization on the ultra-low electrical percolation threshold and on the mechanical behavior of sintered UHMWPE-based nanocomposites, Polymer 111 (2017) 204-213.

[40] R.P. Kusy, Influence of particle size ratio on the continuity of aggregates, Journal of Applied Physics 48 (1977) 5301-5307.

[41] Ye.P. Mamunya, V.V. Davydenko, H. Zois, Dielectric properties of polymers filled with dispersed metals, Polym Polym Compos 10(3) (2002) 219-227.

[42] T.A. Ezquerra, M. Kulescza, C.S. Cruz, F.J. Baltá-Calleja, Charge transport in polyethylene–graphite composite materials, Adv Mater 2(12) (1990) 597-600.

[43] S. Torquato, Random heterogeneous materials. Microstructure and macroscopic properties, Springer, New York, 2012.

[44] H. Tuononen, K. Fukunaga, M. Kuosmanen, J. Ketolainen, K.E. Peiponen, Wiener bounds for complex permittivity in terahertz spectroscopy: case study of two-phase pharmaceutical tablets, Appl Spectrosc 64(1) (2010) 127-131.

[45] K. Lichtenecker, Der elektrische Leitungswiderstand künstlicher und natürlicher Aggregate, Physikalische Zeitschrift 25 (1924) 225-233.

[46] J.K. Carson, S.J. Lovatt, D.J. Tanner, A.C. Cleland, Predicting the effective thermal conductivity of unfrozen, porous foods, J Food Eng 75(3) (2006) 297-307.

[47] H. Chen, V. Ginzburg, J. Yang, Y. Yang, W. Liu, Y. Huang, L. Du, B. Chen, Thermal conductivity of polymer-based composites: Fundamentals and applications, Prog Polym Sci 59 (2016) 41-85.

[48] M.T. Sebastian, H. Jantunen, Polymer–ceramic composites of 0–3 connectivity for circuits in electronics: A Review, Int. J Appl Ceram Technol 7(4) (2010) 415-434.

[49] K. Pietrak, T.S. Wisniewski, A review of models for efective thermal conductivity of composite materials, J Power Techn 95(1) (2015) 14-24.

[50] R.C. Progelhof, J.L. Throne, R.R. Ruetsch, Methods for predicting the thermal conductivity of composite systems: A review, Polym Eng Sci 16(9) (1976) 615-625.

[51] Z.M. Dang, J.K. Yuan, J.W. Zha, T. Zhou, S.T. Li, G.H. Hu, Fundamentals, processes and applications of high-permittivity polymer–matrix composites, Prog Mater Sci 57(4) (2012) 660-723.

[52] Ye. Mamunya, A. Boudenne, N. Lebovka, L. Ibos, Y. Candau, M. Lisunova, Electrical and thermophysical behaviour of PVC-MWCNT nanocomposites, Compos Sci Technol 68 (9) (2008) 1981-1988.

[53] M. Jouni, A. Boudenne, G. Boiteux, V. Massardier, B. Garnier, A. Serghei, Electrical and thermal properties of polyethylene/silver nanoparticle composites, Polym Compos 34 (2013) 778-786.

[54] Sh. Nejad, A review on modeling of the thermal conductivity of polymeric nanocomposites, e-Polymers 25 (2012) 1-38.

[55] S.T. Huxtable, D.G. Cahill, S. Shenogin, L. Xue, R. Ozisik, P. Barone, M. Usrey, M.S. Strano, G. Siddons, M. Shim, P. Keblinski, Interfacial heat flow in carbon nanotube suspensions, Nat Mater 2(11) (2003) 731-734.

[56] S. Hida, T. Hori, T. Shiga, J. Elliott, J. Shiomi, Thermal resistance and phonon scattering at the interface between carbon nanotube and amorphous polyethylene, Int J Heat Mass Tran 67 (2013) 1024-1029.

[57] J. Gu, Z. Lv, Y. Wu, Y. Guo, L. Tian, H. Qiu, W. Li, Q. Zhang, Dielectric thermally conductive boron nitride/polyimide composites with outstanding thermal stabilities via in-situ polymerization-electrospinning-hot press method, Compos Part A Appl Sci Manuf 94 (2017) 209-216.

[58] X. Yang, L. Tang, Y. Guo, C. Liang, Q. Zhang, K. Kou, J. Gu, Improvement of thermal conductivities for PPS dielectric nanocomposites via incorporating NH2-POSS functionalized nBN fillers, Compos Part A Appl Sci Manuf 101 (2017) 237-242.

[59] X. Yang, Y. Guo, X. Luo, N. Zheng, T. Ma, J. Tan, C. Li, Q. Zhang, J. Gu, Self-healing, recoverable epoxy elastomers and their composites with desirable thermal conductivities by incorporating BN fillers via in-situ polymerization, Compos Sci Technol 164 (2018) 59-64.

[60] Y. Guo, Z. Lyu, X. Yang, Y. Lu, K. Ruan, Y. Wu, J. Kong, J. Gu, Enhanced thermal conductivities and decreased thermal resistances of functionalized boron nitride/polyimide composites, Compos Part B-Eng 164 (2019) 732-739.

[61] Ye.P. Mamunya, V.V. Levchenko, I.M. Parashchenko, E.V. Lebedev, Thermal and electrical conductivity of the polymer-metal composites with 1D structure of filler formed in a magnetic field, Polymer J (Ukraine) 38(1) (2016) 3-17.

[62] N. Shenogina, S. Shenogin, L. Xue, P. Keblinski, On the lack of thermal percolation in carbon nanotube composites, Appl Phys Lett 87(13) (2005) 133106.